URSI GASS 2021, Rome, Italy, 28 August - 4 September 2021

A High-Impedance Surface for Improving Performance of Microwave Imaging Antennas for Biomedical Applications

Maria Conte[(1)], Elisa Giampietri[(1), (2)], Danilo Brizi*[(1), (2)], Agostino Monorchio[(1), (2)]
(1) Department of Information Engineering, University of Pisa, Pisa, 56122, Italy
(2) Consorzio Nazionale Interuniversitario per le Telecomunicazioni (C.N.I.T.), Pisa, 56124, Italy

Abstract

In this paper we introduce a high impedance surface for improving performance of antennas employed in biomedical Microwave Imaging (MWI). We first design a standard bow-tie antenna, commonly adopted in MWI, by using a commercial numerical electromagnetic solver. Then, we develop the high impedance surface to be placed behind the proposed bow-tie. The numerical simulations demonstrated that the use of the high impedance surface implies an excellent improvement in the electromagnetic energy delivery inside a biological phantom, quantifiable by a significantly higher coupling between two opposite radiating elements. This study can pave the way in the use of high impedance surfaces within the uprising topic of Microwave Imaging for clinical purposes.

1 Introduction

Microwave Imaging (MWI) has strongly emerged in the last decades as a promising diagnostic modality, especially suited for breast cancer detection and for brain stroke classification [1]-[2]. The potential advantages of MWI in these specific diagnostic areas are significantly important; indeed, the technique is perfectly safe for human health, not using any kind of ionizing radiation and it is completely non-invasive. Moreover, if we especially relate to breast cancer, this modality is more comfortable for the patient, because the breast crushing, typical of x-ray mammography, is not required. Finally, MWI is extremely less expensive than ordinary imaging modalities, thus it can be adopted easily in any hospital facility [3].

Traditionally, MWI can be performed according to two main modalities, i.e. by using a broadband signal (radar-based techniques) or by employing a single-frequency exciting pulse (common in 3D reconstruction imaging) [2]. In any case, one important feature to be achieved in order to obtain a sufficient imaging quality consists in good radiating properties of the employed antennas within the tissue under investigation.

In particular, in a common arrangement, an array of radiating elements is adopted. Thus, each radiating element is used to excite tissues and the transmitted and scattered radiation is received by the other elements of the array. In this way, image reconstruction can be accomplished [1]-[3]. Therefore, a major requirement is the antenna capability to deliver as much electromagnetic energy as possible inside tissues, consequently increasing the signal-to-noise ratio. However, it is a matter of fact that the penetration depth becomes lower when the frequency increases; nonetheless, higher operative frequencies are desirable to achieve an acceptable spatial resolution. For this reason, a significant effort in the literature has been directed to find technical solutions to improve the energy penetration inside tissues. One adopted possibility is using an impedance matching liquid (as water) to be interposed between the antenna and the tissues [4]. Although very straightforward, nevertheless the matching layer is cumbersome and not easily integrable within these systems. Therefore, the use of metamaterials and metasurfaces was also proposed [4]-[5]. This methodology is very promising because especially metasurfaces can be realized as very thin impedance sheets able to be easily inserted between the antenna and the tissues.

To the best of our knowledge, in this paper we propose for the first time the use of high impedance surfaces (HIS) to enhance the energy deposition inside biological tissues for clinical applications of microwave imaging [6]. We design, through a numerical electromagnetic solver, a common antenna for MWI, i.e. a bow-tie, and a suitable HIS, working at 2.56 GHz. We prove through full-wave simulations that a HIS slab placed behind the radiating element is able to significantly increase the coupling between two opposite radiating elements, even in presence of a biological phantom.

The paper is organized as follows. Section 2 is devoted to the design of the bow-tie antenna along with the HIS; in Section 3, we present and discuss the obtained results. Finally, Conclusions follow.

2 Proposed Numerical Test-case

2.1 Adopted Bow-tie Model

In order to design and verify our proposed solution, we conceived a numerical test-case, exploiting an electromagnetic solver based on the Finite Elements Method (Ansys Electronics Desktop, Ansys Inc., Canonsburg, PA, USA).

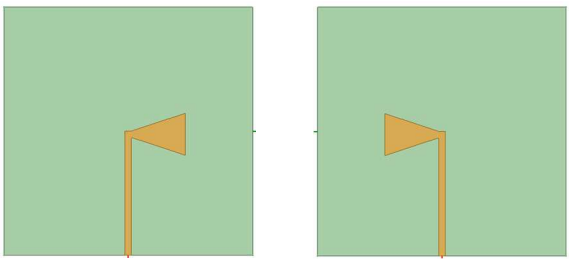

(a) (b)

Figure 1. CAD model of the employed bow-tie antenna: (a) upper layer; (b) bottom layer. The antenna is layered onto a 0.8 mm thick FR4 substrate (ε_r = 4.4, tanδ = 0.02).

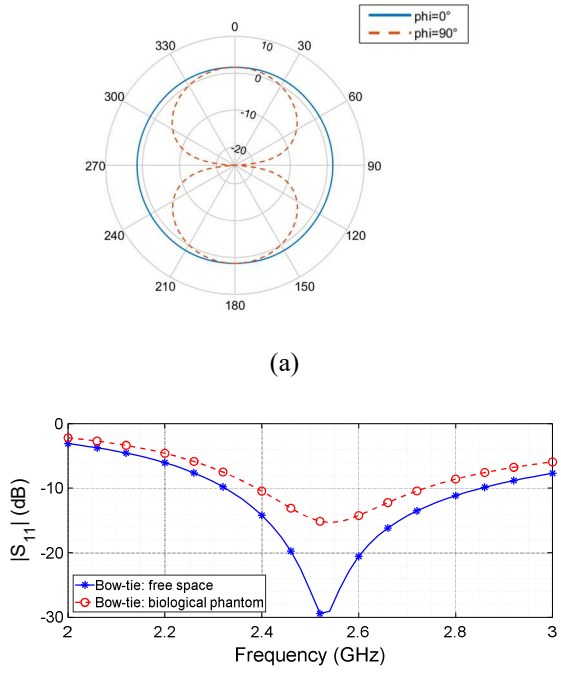

Figure 2. Radiating performance of the proposed bow-tie antenna: (a) radiation patterns in dB for radiation planes at ϕ=0° and ϕ=90°; (b) Antenna S_{11} parameter in free space (blue continuous line) and in the presence of the biological phantom (red dashed line).

Initially, we realized a traditional PCB etched bow-tie antenna (Fig. 1). Specifically, the isosceles triangle element of the antenna presents a height of 17 mm, whereas the feeding strip line is 40 mm long and 2 mm wide. The overall antenna has been layered onto a 0.8 mm thick FR4 substrate (ε_r = 4.4, tanδ = 0.02).

The dimensions of the antenna, the thickness and typology of the substrate have been chosen through an optimization process in order to match the desired operative frequency of about 2.56 GHz. Fig. 2(a) shows the antenna radiation pattern for the two main geometrical planes, confirming the typical behavior of a classical bow-tie configuration.

In addition, in order to adopt a more realistic scenario, we also designed a biological phantom, placed 15 mm away from the antenna. For simplicity, the phantom was realized as a homogeneous cuboid (90 mm × 90 mm × 70 mm) which shows the brain average dielectric properties (ε_r = 43, tanδ = 0.27). Fig. 2 (b) reports the S_{11} antenna parameter in free space and in the presence of the phantom; as evident, the designed antenna is able to correctly perform at the desired operative frequency in both the conditions.

2.2 Adopted HIS model

The next step was directed to design a suitable high impedance surface to be inserted behind the proposed bow-tie antenna. We performed a preliminary study, analyzing the single unit-cell and exploiting the periodic boundary condition to obtain the theoretical response of the ideal infinite 2D structure.

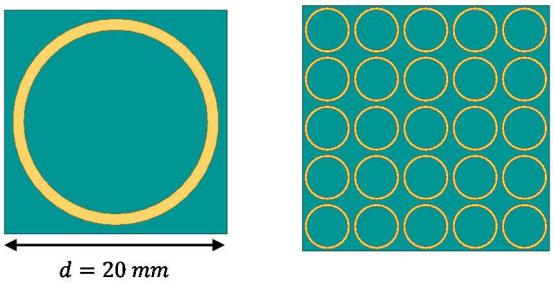

Figure 3. CAD model of the proposed HIS slab: (a) single unit-cell; (b) the realized 5×5 metasurface.

As shown in Fig. 3(a), the selected unit-cell is a metal loop with a periodicity of 20 mm; the PEC loop is made of a 1 mm wide strip, layered on a 1.6 mm thick dielectric substrate (ε_r = 6.15). The structure is backed by a ground plane. Fig. 4 reports the phase of the reflection coefficient for a TE polarized incident plane wave; it can be pointed out that the HIS behavior (first zero in the phase diagram) is present at the desired frequency range.

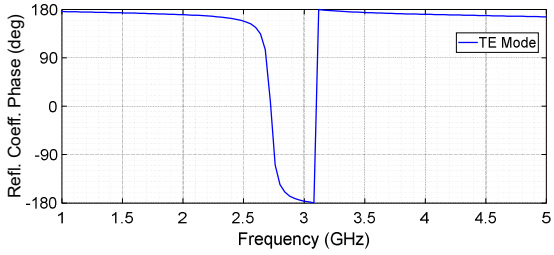

Figure 4. HIS reflection coefficient phase obtained for an impinging TE polarized plane wave. The first zero-crossing is around 2.56 GHz, as desired.

At this point, we realized the design of the actual HIS to be placed behind the bow-tie antenna, considering a 5×5 matrix of elements as a compromise between compactness and performance enhancement (Fig. 3(b)).

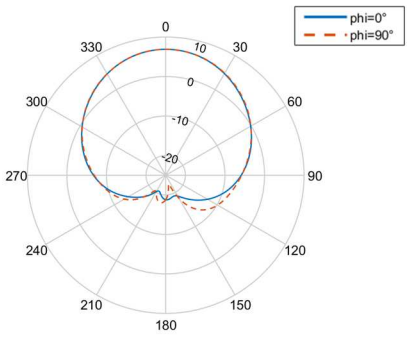

(a)

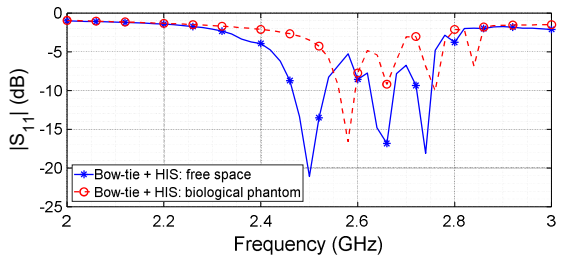

(b)

Figure 5. Radiating performance of the bow-tie antenna backed by the proposed HIS: (a) radiation patterns in dB for geometrical planes at ϕ=0° and ϕ=90°; (b) Antenna S_{11} parameter in free space (blue continuous line) and in the presence of the biological phantom (red dotted line).

Finally, the HIS was placed behind the bow-tie antenna, choosing through an optimization procedure the distance from it (i.e., 3.5 mm below). Fig. 5(a) depicts the bow-tie radiation pattern in presence of the proposed HIS; it can be highlighted the dramatic reduction of the undesired back-radiation and a higher antenna gain, thus confirming the optimal HIS behavior [6]. Moreover, in Fig. 5(b) we reported the S_{11} parameter of the bow-tie antenna backed by the HIS, for the free space case and in presence of the previously described biological load. The biological phantom produces a slight shift of the antenna resonant frequency (at about 2.56 GHz), nonetheless remaining within the desired operative range.

3 Results

Once designed the bow-tie antenna and the HIS in order to achieve the desired operating frequency, we performed full-wave simulations to compare two different set-ups. The first one consists of two equal and opposite bow-tie antennas separated by the adopted biological phantom (Fig. 6(a)). Each antenna is placed 15 mm away from the phantom. The second configuration is analogous to the first one, but, in addition, each antenna is backed by the designed HIS (placed, in turn, 3.5 mm behind the bow-tie, Fig. 6(b)).

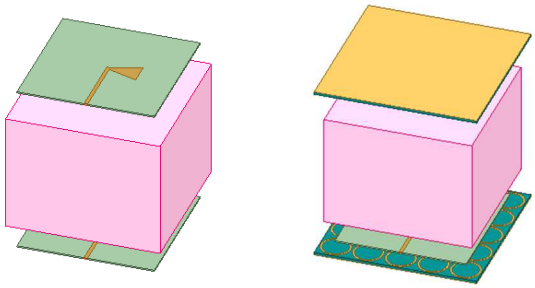

(a) (b)

Figure 6. Tested configurations: (a) two opposite bow-tie antennas interleaved by the biological phantom; (b) the bow-tie antennas are backed by the designed HIS slab.

The comparison is directed to evaluate which configuration has the better coupling, i.e. the better e.m. energy transmission inside the tissues. As Fig. 7 demonstrates, the design where the HIS is employed is able to significantly outperform the simple antenna-antenna configuration in terms of coupling (+ 12 dB). Moreover, as already pointed out before, the HIS presence can significantly reduce the bow-tie undesired back radiation. Thus, these results validate the potentiality of inserting a high impedance surface in MWI systems to increase their performance.

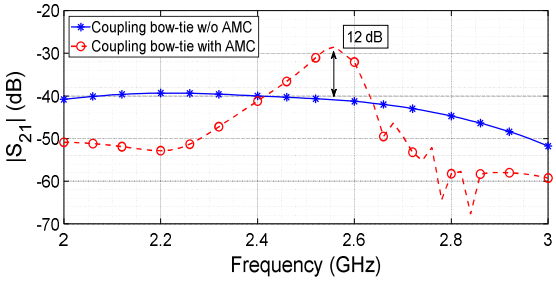

Figure 7. S_{21} parameter comparison between the two configurations described in Fig. 6. It can be pointed out the coupling enhancement produced by the HIS presence.

4 Conclusions

In this paper, we showed that the use of high impedance surfaces for biomedical Microwave Imaging applications can enhance the overall system performance. We first designed a common antenna typology adopted in MWI, i.e. the bow-tie antenna, operating at 2.56 GHz. Then, we conceived the HIS to be placed behind the antenna. Through accurate full-wave simulations, we demonstrated that the coupling between two opposite radiating elements separated by a biological phantom significantly increases by employing a properly designed HIS, implying an enhancement of the e.m. energy delivered to the tissues, and, consequently, of the signal-to-noise ratio. Future development will be directed to further analyze this preliminary technical solution and to fabricate a prototype to be experimentally tested.

5 References

1. M. Persson et al., “Microwave-based stroke diagnosis making global prehospital thrombolytic treatment possible,” *IEEE Trans. Biomed. Eng.*, **61**, 11, pp. 2806–2817, 2014.

2. R. Chandra, H. Zhou, I. Balasingham, and R. M. Narayanan, “On the opportunities and challenges in microwave medical sensing and imaging,” *IEEE Trans. Biomed. Eng.*, **62**, 7, pp. 1667–1682, 2015.

3. M. A. Aldhaeebi, K. Alzoubi, T. S. Almoneef, S. M. Bamatraf, H. Attia, and O. M Ramahi, “Review of Microwaves Techniques for Breast Cancer Detection,” *Sensors*, **20**, 8, p. 2390, 2020.

4. E. Razzicchia et al., "Feasibility study of enhancing microwave brain imaging using metamaterials", *Sensors,* **19**, 24, pp. 54-72, 2019.

5. M. Islam et al., "Microwave imaging sensor using compact metamaterial UWB antenna with a high correlation factor", *Materials*, **8**, 8, pp. 4631-4651, 2015.

6. F. Costa, S. Genovesi and A. Monorchio, "On the Bandwidth of High-Impedance Frequency Selective Surfaces", *IEEE Antennas and Wireless Propagation Letters*, **8**, pp. 1341-1344, 2009, doi: 10.1109/LAWP.2009.2038346.